



# Adsorption isotherms and thermodynamic properties of a butyl functionalized hydrophobic macroporous cryogel

Thainnane Silva Paiva<sup>1</sup> · Rui Gomes Nascimento<sup>1</sup> · Lizzy Ayra Alcântara Veríssimo<sup>2</sup> · Renata Cristina Ferreira Bonomo<sup>1</sup> · Cristiane Martins Veloso<sup>1</sup> · Jaime Vilela de Resende<sup>2</sup> · Rafael da Costa Ilhéu Fontan<sup>1</sup>

Received: 22 April 2021 / Revised: 5 August 2021 / Accepted: 3 October 2021 / Published online: 18 October 2021  
© Associação Brasileira de Engenharia Química 2021

## Abstract

The production of polymeric monolithic structures with highly interconnected pores has attracted the attention of researchers, since developing adsorbents that allow for purifying biomolecules while maintaining their bioactivity is essential in several fields. The monoliths are versatile in their use and functionalization possibilities. A novel approach was used in the operation with butyl amine of polyacrylamide cryogels with alkyl glycidyl ether for use in hydrophobic interaction chromatography. The results of the FTIR and TGA thermogravimetric spectroscopy analyses indicated success and scanning electron microscopy analyses confirmed a macroporous structure. Values found for the swelling capacity, degree of expansion and porosity corroborated the literature and the high permeability demonstrated the ease of flow in the produced matrices. We evaluated the adsorption of bovine serum albumin (BSA) in the adsorbent. The Langmuir model adequately adjusted to the data obtained and non-linear van't Hoff analysis was used to determine the variation of the thermodynamic properties for the adsorption process, which occurred spontaneously ( $\Delta G_{\text{ads}} \leq -20.0 \text{ kJ mol}^{-1}$ ) for all temperatures. We verified that the maximum adsorption capacity ( $q_{\text{max}}$ ) ranged from 696.28 to 1735.56  $\text{mg g}^{-1}$ . The developed matrix showed potential for application in capture processes by hydrophobic interaction.

**Keywords** Hydrophobic interaction · Enthalpy · Entropy · Gibbs free energy

## Introduction

The development of new bioseparation strategies and biotechnological processes, including chromatographic techniques, has grown considerably in the chemical and food industry (Wen et al. 2020). Chromatography is a physical–chemical process used to separate biomolecules, with the aim of isolating and purifying one or more compounds of interest in a given solution, leading to the appropriate purity for its specific use (Jungbauer 2005). Separation and purification can occur in several ways, including an affinity for compounds of interest, ion exchange between available

molecules and hydrophobic interactions (Wen et al. 2020; Jungbauer 2005).

Hydrophobic interaction chromatography has advantages over other types of chromatography, as it achieves rapid separation with little product degradation and high purification levels (Türkmen and Denizli 2014). This technique uses the hydrophobic regions of proteins to separate them. According to Fontan et al. (2018), the process is based on reversible interactions formed between the hydrophobic zones present on the surface of the protein and the hydrophobic ligand of a chromatographic resin. When salt is added to the protein solution, the hydrophobic regions are exposed because of the disruption of the water solvation layer of the proteins. Thus, proteins tend to interact more with the hydrophobic matrix, which makes separation possible (Chen et al. 2008).

Among the existing chromatographic resins, macroporous cryogels are particularly interesting for use in purification processes of macromolecular biocomposites, such as proteins from less clarified media, as they reduce the number of required steps (Mol et al. 2017). Cryogels are matrices

✉ Rafael da Costa Ilhéu Fontan  
rafaelfontan@yahoo.com.br; rafaelfontan@uesb.edu.br

<sup>1</sup> Processes Engineering Laboratory, State University of Southwest of Bahia, BR-415, km 03, Itapetinga, BA 45700-000, Brazil

<sup>2</sup> Department of Food Science, Federal University of Lavras, Lavras, MG, Brazil

of polymeric gels formed at freezing conditions (formed ice crystals act as porogenic agents, giving shape and size to the pores created after thawing). This process generates continuous and interconnected macropores that provide low resistance, allowing easier flow (Plieva et al. 2004; Ertürk and Mattiasson 2014). These highly porous polymeric materials can be produced from different monomers and present a wide variety of morphologies and porosities (Plieva et al. 2009; Kumar et al. 2006). Chemical and physical modifications can be made to the cryogel matrix to increase its selectivity according to the product of interest to be purified, thus increasing the efficiency of the separation processes (Kumar et al. 2006; Ingavle et al. 2015; Gonçalves et al. 2016). With the introduction of new chemical structures (hydrophobic groups) on the surface, it is possible to obtain stationary phases that interact more or less specifically with a particular protein (Ertürk and Mattiasson 2014).

In order to improve the use of cryogels, several methodologies for functionalizing their surfaces have been studied (Andaç et al. 2016). These functionalizations are performed by inserting reactive groups, which interact with the amine ( $\text{NH}_2$ ), thiol (SH), and hydroxyl (OH) groups. Therefore, it is important to have specific functional groups in the material structure. Epoxy groups, such as allyl-glycidyl ether (AGE), are an example of functional groups of monomers. The epoxy groups can be used in a future reaction step as an anchoring group to immobilize specific ligands or to improve properties such as range of pH stability, hydrophilicity, hydrophobicity, or activation temperature (Savina et al. 2005). The glutaraldehyde method is widely used in functionalizing the cryogel surfaces containing these monomers, where the adsorbent containing reactive epoxy groups (epoxy-activated) is initially converted to the amine-activated form by means of epoxy group reactions with reagents containing an amine group, such as ethylenediamine (Ingavle et al. 2015). The amine-activated monolith reacted with the glutaraldehyde, forming an aldehyde-activated monolith capable of reacting with amine radicals of the linker molecule. The support is used in the same manner as with the Schiff base method (Kumar et al. 2006) but has the advantage of forming a long spacer arm between the monolith and the ligand. This avoids possible steric hindrance effects (Savina et al. 2005; Guo et al. 2014), which may result in higher ligand immobilization capacity to purify the target molecule.

To ensure the radicals of interest are linked to the chromatographic matrix to give it desirable interaction characteristics without significantly affecting operational aspects (such as the presence of macropores) it is important to characterize the material produced using tools such as FTIR spectroscope, TGA thermogravimetric analysis and scanning electron microscopy (Plieva et al. 2004). In addition to the physical characteristics, it is necessary to know the

adsorptive behavior of the material produced. For this, it is essential to determine the adsorption isotherms and use thermodynamic analysis to obtain the balance data regarding protein retention in the chromatographic column (Ertürk and Mattiasson 2014; Plieva et al. 2008; Kumar et al. 2006).

Thus, the objective of the work was to develop and characterize a butyl functionalized hydrophobic macroporous cryogel concerning physical, chemical, adsorptive and thermodynamics aspects.

## Materials and methods

### Reagents

The following materials were used for cryogel production: acrylamide (AAM), bis-acrylamide (BAAM), butylamine, *N,N,N',N'*-tetramethylethylenediamine (TEMED), ammonium persulfate (APS), allyl-glycidyl-ether (AGE), ethylenediamine, sodium phosphate and sodium borohydride. All reagents used were of PA-ACS purity grade and acquired from Sigma-Aldrich (St. Louis, USA). BSA, purity grade  $\geq 96\%$ , was acquired from Sigma-Aldrich (St. Louis, USA).

### Monolithic cryogel synthesis

The cryogels were synthesized according to Kumar et al. (2006) and Yao et al. (2006), with modifications. Initially, 4.4 g of AAM, 1.2 g of BAAM and 1.4 g of AGE were weighed, making a final monomer concentration of 7% w/v for a final solution volume of 100 mL. Polymerization was done by adding of 140  $\mu\text{L}$  of APS ( $0.5 \text{ mg mL}^{-1}$ ) and 91  $\mu\text{L}$  of TEMED. The mixture was stirred in an ice bath and poured into 5 mL plastic syringes. The syringes were sealed and immersed in an ethyl alcohol bath at  $-12 \text{ }^\circ\text{C}$  for 24 h. The formed cryogels were then thawed at cooling temperature ( $5 \text{ }^\circ\text{C}$ ) and the syringes were placed open in a  $60 \text{ }^\circ\text{C}$  oven until the cryogels were completely dry. The ends of the cryogel pieces were cut to remove defective parts and were washed with 150 mL of distilled water using a peristaltic pump at a flow rate of  $1.5 \text{ mL min}^{-1}$ . The cryogels were again dried in an oven and the masses were determined in an analytical balance.

### Functionalization of cryogels for adsorption by hydrophobic interaction

For the functionalization process with butylamine, the glutaraldehyde method in a batch system was adapted from Da Silva et al. (2019). The dry cryogels, about 3 cm in height, 1 cm in diameter, and an average weight of 250 mg (dry weight), were placed under rotating agitation at 25 RPM

at all steps of the process, using closed 20 mL syringes. At each step, i.e. when the solution was changed, the cryogels were gently compressed by hand to remove excess solution from the previous stage.

The cryogels were placed in contact with 20 mL of methyl alcohol for 2 h. They were kept in contact with 20 mL of distilled water, followed by contact with 20 mL of 0.05 mol L<sup>-1</sup> pH 6 sodium phosphate buffer (PBS), both with a contact time of 1 h. They were immersed in 20 mL of 0.5 mol L<sup>-1</sup> ethylenediamine in PBS and kept under stirring for 14 h at room temperature (25 ± 2) °C.

After this step, the cryogels were washed with distilled water and then immersed in 20 mL of PBS, with each stage lasting 1 h. The cryogels were placed in contact with 20 mL of 5% glutaraldehyde solution in PBS, at a controlled temperature of (12.0 ± 0.5) °C for 5 h. The cryogels were rinsed twice with 20 mL distilled water for 30 min to remove excess glutaraldehyde. The aldehyde-activated cryogels were kept in contact with 20 mL of 10 mg mL<sup>-1</sup> butylamine solution in PBS for 14 h at room temperature (25 ± 2) °C.

The matrices were immersed in 20 mL of PBS for 1 h and then in 20 mL of 0.1 mol L<sup>-1</sup> sodium borohydride solution in PBS for 60 min with the flasks open. Finally, to block unreacted epoxy and carboxyl radicals, the cryogels were washed with 20 mL of distilled water, followed by 20 mL of 0.1 mol L<sup>-1</sup> ethanolamine in PBS and again 20 mL of distilled water, with the last three steps lasting 1 h each. After the inclusion of functional groups, the cryogels were placed in an oven at 60 °C and a supermacroporous monolithic adsorbent column with hydrophobic interaction was obtained after drying.

### Cryogel characterization

To characterize the cryogel produced and later functionalized, the analyses were carried out following the methodologies proposed by Savina et al. (2005) for swelling capacity (S), Fontan et al. (2018) for degree of expansion (ED), and Plieva et al. (2004, 2009) for porosity. Scanning electron microscopy (SEM), Fourier transform infrared spectroscopy (FTIR) and thermogravimetric analysis (TGA) were performed using the methodologies proposed by Da Silva et al. (2019).

### Adsorption isotherms

Isotherms data were obtained using the batch method as reported by Carvalho et al. (2013), Veríssimo et al. (2017), and Oliveira et al. (2019). The experimental data were fitted to the Langmuir (1916) model. Aqueous solutions (4 mL) containing different amounts of BSA (0.1–15 mg mL<sup>-1</sup> initial concentration) in sodium phosphate buffer (0.03 mol L<sup>-1</sup>; pH 7.2) added to 2.0 mol L<sup>-1</sup> sodium sulfate were incubated

in Falcon plastic tubes with 30 mg cryogel under agitation and placed in a BOD oven for 24 h. The adsorption isotherms were obtained experimentally, in triplicate, at temperatures of 298.15, 308.15, 318.15, and 328.15 K. After 24 h, the solution was separated from the supernatant by centrifugation at 1500g for 10 min. The Bradford (1976) method was used to quantify the protein in the initial solution and the supernatant, with a spectrophotometer reading at 595 nm. The amount of adsorbed BSA was determined according to Eq. (1):

$$q = \frac{(C_0 - C) \cdot V}{m} \quad (1)$$

where q is the amount of protein adsorbed in dry cryogel (mg protein/g cryogel); C<sub>0</sub> and C are the initial and final protein concentrations (mg mL<sup>-1</sup>); V is the solution volume (mL); and m is the dried cryogel mass (g).

### Thermodynamic analysis

From the adsorption equilibrium data, a van't Hoff analysis was performed to determine the thermodynamic parameters ΔH<sub>ads</sub><sup>°</sup>, ΔS<sub>ads</sub><sup>°</sup> and ΔG<sub>ads</sub><sup>°</sup>, using Eqs. (2) and (3), and the methodology proposed by Bonomo et al. (2006) and Ueberbacher et al. (2010).

$$\ln K' = \frac{-\Delta H^{\circ} ads}{RT} + \frac{\Delta S^{\circ} ads}{R} + \theta \quad (2)$$

$$\ln K' = a + \frac{b}{T} + \frac{c}{T^2} + \theta \quad (3)$$

With K' being the equilibrium constant, ΔH<sub>ads</sub><sup>°</sup> and ΔS<sub>ads</sub><sup>°</sup> the changes in enthalpy and standard entropy of adsorption, R the universal constant of gases, T the temperature and θ a system constant that depends on the ratio between the phases.

## Results and discussion

### Synthesis, functionalization and characterization of the matrices produced

The produced matrices presented a rigid, spongy and homogeneous structure, with a cylindrical shape due to the syringe mold. The control cryogels presented a white color while the functionalized cryogels were yellow (Fig. 1). The yellowish color was due to the formation of Schiff bases in the functionalization process, which is a precursor of the pigments formation from the Maillard reaction (Da Silva et al. 2019). When hydrated, they presented desirable properties, such

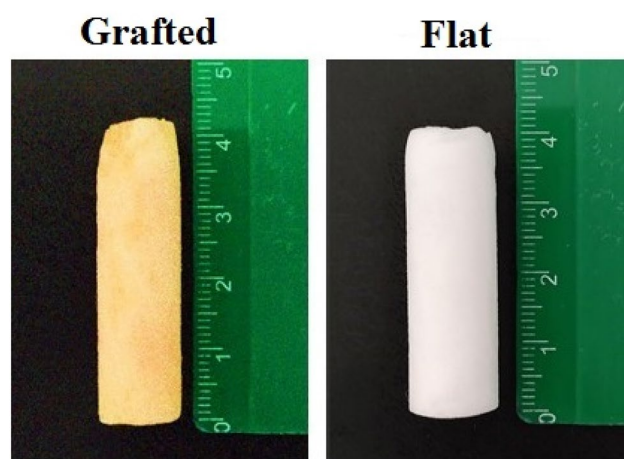


**Fig. 1** Image of the control and functionalized (grafted) cryogels produced in the experiment

**Table 1** Characterization of the control and functionalized cryogels

Parameter	Control	Functionalized
Swelling capacity ( $\text{kg kg}^{-1}$ )	$10.89 \pm 0.31$	$10.75 \pm 1.43$
Degree of expansion ( $\text{L kg}^{-1}$ )	$10.87 \pm 1.87$	$10.40 \pm 3.93$
Fraction of macropores*	$0.688 \pm 0.006$	$0.647 \pm 0.005$
Meso and micropore fraction*	$0.183 \pm 0.005$	$0.216 \pm 0.005$
Binding water fraction	$0.045 \pm 0.009$	$0.051 \pm 0.020$
Dry polymer fraction	$0.084 \pm 0.002$	$0.086 \pm 0.010$
Total porosity	$0.871 \pm 0.011$	$0.863 \pm 0.010$

Average values obtained for swelling capacity (S), degree of expansion (ED), and pore fractions of the matrices produced

\*Significant difference between treatments in t test at 5% significance level

as high porosity. The cryogels maintained their structural characteristics after being dried and rehydrated.

Table 1 shows the results obtained for the swelling capacity (S), degree of expansion (DE) and pore fractions. The swelling capacity of the produced cryogels did not differ statistically ( $p > 0.05$ ), indicating the activation did not promote a change in the cryogel structure in the ability to hydrate (Ertürk and Mattiasson 2014). The degree of expansion (DE) decreased in the functionalized cryogel, since the incorporation of hydrophobic monomer in a cryogenic network increased the hydrophobicity of the prepared cryogels. The S and DE values obtained in this work are within the ranges reported for polyacrylamide cryogels in several works (Sahiner 2018; Ingavle et al. 2015; Osman et al. 2019; Fontan et al. 2018; Mol et al. 2017; Da Silva et al. 2019; Gonçalves et al. 2017). For total porosity, the activated and control cryogels showed no significant difference ( $p > 0.05$ ) between them. With the functionalization however, there was a reduction

in the fraction of macropores and mesopores, with a small elevation in the fraction of smaller pores in the inclusion of the spacer arms because of the polymerization potential presented by glutaraldehyde used in this process. This fact caused some of the macropores to behave like micro and mesopores because they were partially obstructed, which affected the flow dynamics inside them. The values found were consistent with those observed in other studies involving polyacrylamide cryogels (Demirci and Sahiner 2021; Bayramoglu and Arica 2021; Da Silva et al. 2019; Gonçalves et al. 2017; Veríssimo et al. 2017; Wang et al. 2013).

Regarding the morphological evaluation of the produced matrices, scanning electron microscopy (SEM) analysis was used (Fig. 2). The matrices presented a homogeneous structure, with large and interconnected pores in the control (A to B) and functionalized (C and D) matrices, following what has been reported by several authors (Gonçalves et al. 2017; Veríssimo et al. 2017; Nascimento et al. 2019). The pore size was large enough for the passage of both macromolecules, as well as microbial cells, cellular fragments and even concentrated and particulate solutions, which facilitate purification processes with fewer steps (Gonçalves et al. 2017; Veríssimo et al. 2017).

FTIR analysis was used to evaluate the inclusion of characteristic functional groups during the functionalization process. The spectra obtained are presented in Fig. 3.

In both structures, a strong band characteristic of the C=O group stretched from AAm and BAAM used in the cryogel synthesis process can be observed in the infrared region ( $1650 \text{ cm}^{-1}$ ). In studies using polyacrylamide cryogel, FTIR spectra show strong bands in the same wavelength region (Asgari et al. 2014; Veríssimo et al. 2017; Coates, 2006).

Other specific bands were observed in the  $920$  and  $1067 \text{ cm}^{-1}$  regions in functionalized cryogels and this suggests the presence of functional amine groups, due to the presence of immobilized butylamine molecules in the cryogel. The band at  $1100 \text{ cm}^{-1}$  suggests the presence of C–O present in epoxy radicals from the AGE (Da Silva et al. 2019). Another important observation was in the range between  $1190$  and  $1250 \text{ cm}^{-1}$  of the non-activated cryogel, where there was a band at  $1235 \text{ cm}^{-1}$  that disappeared after activation. The reference band may be associated with the presence of C–O present in alcohol or of C–N bonds of amine groups. (Veríssimo et al. 2017; Coates 2006).

Thermogravimetric analysis was performed and the results are shown in Fig. 4.

A total of three thermal events can be observed between the two polymeric matrices. At temperatures between  $50$  and  $100 \text{ }^\circ\text{C}$ , weight loss occurs, which was attributed to water evaporation, demonstrating that the cryogel contains a large amount of water bound to the polymer. The structure thermally stabilized at approximately  $652 \text{ }^\circ\text{C}$ . Thus, the

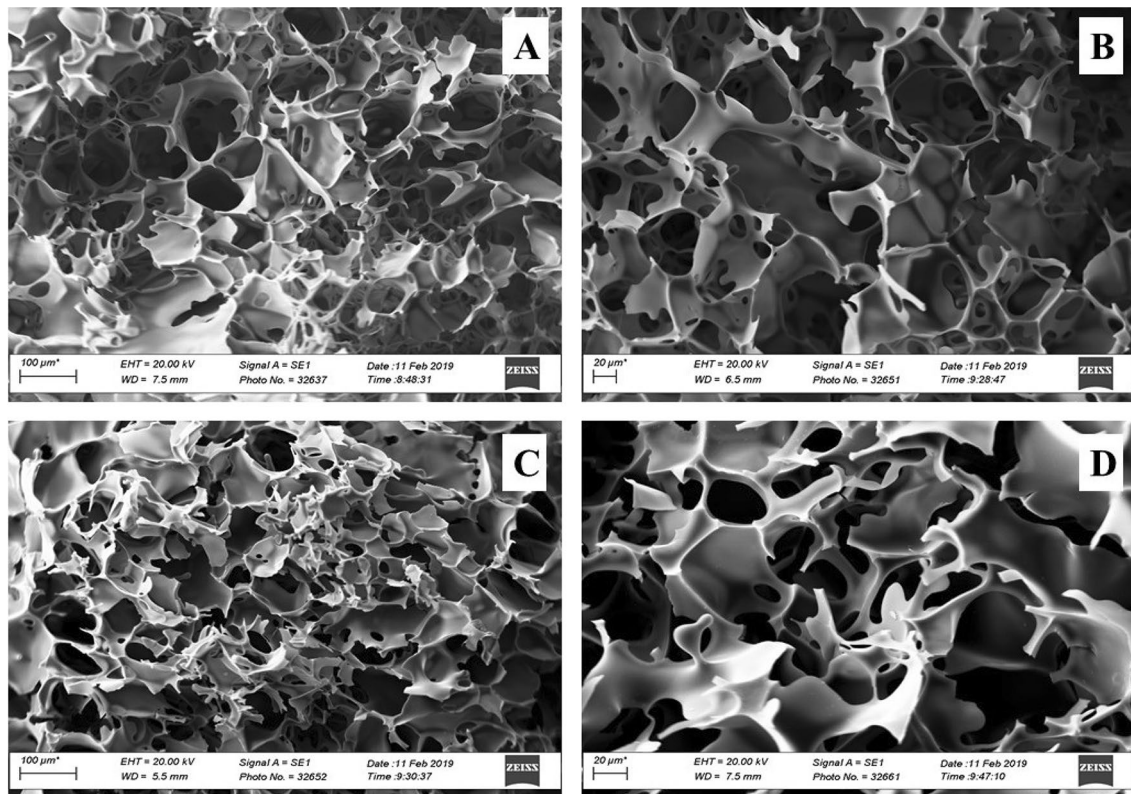


**Fig. 2** SEM micrographs of the cryogel matrices. Control **A**  $\times 250$  and **B**  $\times 500$ . Functionalized **C**  $\times 250$  and **D**  $\times 750$

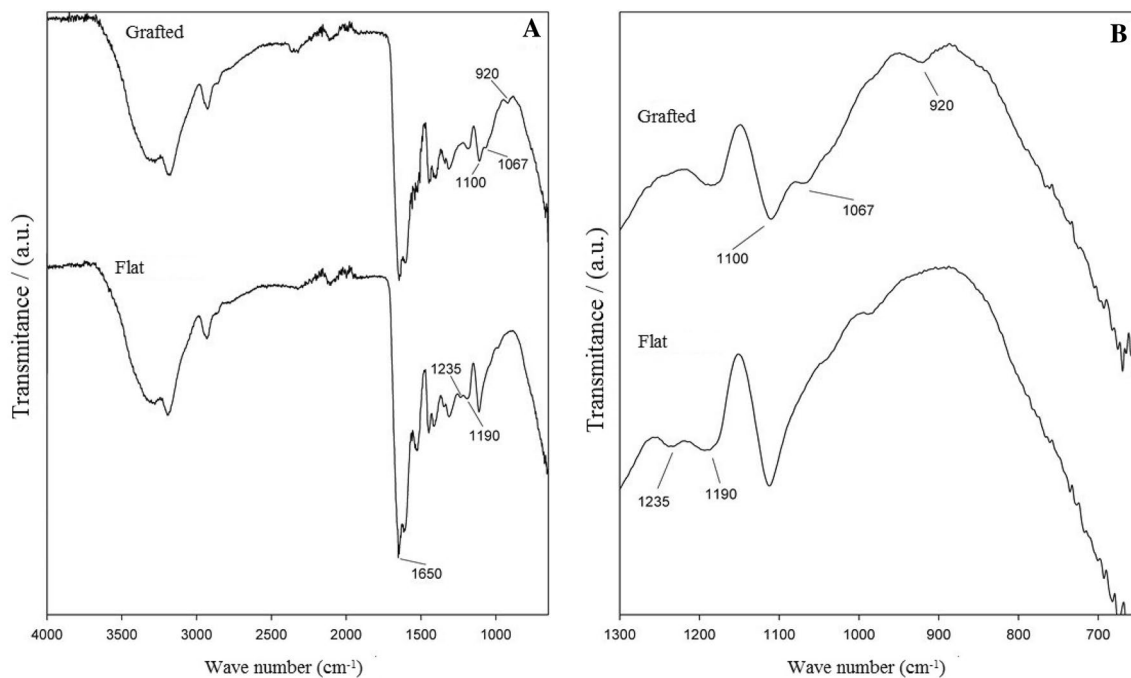


**Fig. 3** FTIR spectra of the cryogels produced. **a** Spectrum from  $650$  to  $4000$   $\text{cm}^{-1}$ . **b** Emphasis on the  $650$ – $1300$   $\text{cm}^{-1}$  region to show the differences between the control and functionalized (grafted) cryogels

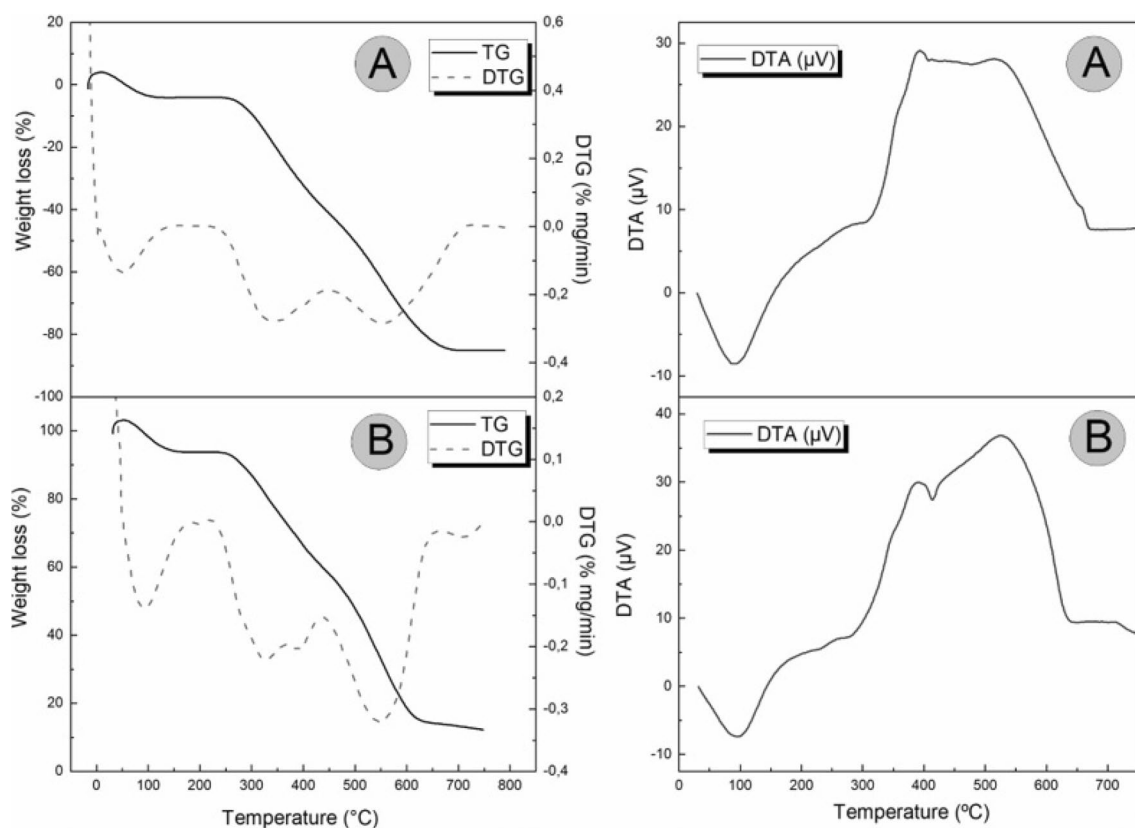


**Fig. 4** TGA curves of the control (A) and functionalized cryogels (B)

thermograms of the cryogels followed the changes during the degradation process of the compounds present in the polyacrylamide monolith. During the thermal degradation of the components in the cryogels, an endothermic peak was observed at temperatures below 100 °C, which was attributed to the losses of free and polymer-bound water and other volatile species. Above 200 °C, a broad exothermic peak between 270 and 400 °C was observed, resulting from the degradation of polyacrylamide for both the activated and control cryogels (Fontan et al. 2018; Mol et al. 2017). An exothermic peak was observed between 415 and 580 °C, which could be associated to degradation of a more crosslinked structure due to glutaraldehyde interactions in spacer arms formed in the functionalization process. (Rimdisit et al. 2012).

### Adsorptive behavior

Figure 5 shows the experimental adsorption isotherms of BSA in hydrophobic cryogel, considering the effect of temperatures of 298.15, 308.15, 318.15 and 328.15 K.

The adsorptive capacity of the protein decreased with increasing temperature. The temperature effect is a complex phenomenon, which can affect both the physical–chemical

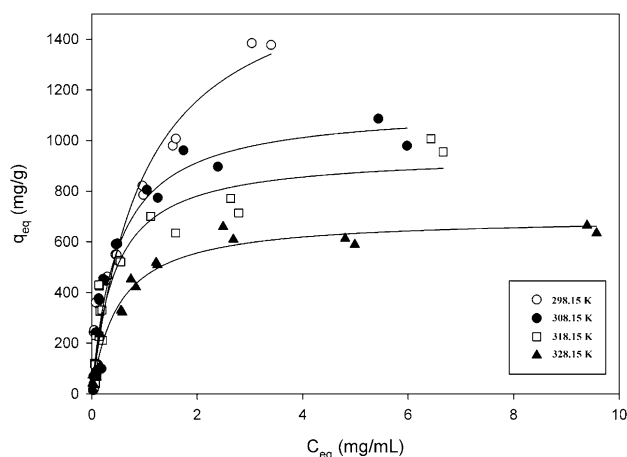


**Fig. 5** Experimental data and predicted values by the Langmuir model (—), at different temperatures

properties of the adsorbent and the properties of the solute, such as conformational and configurational changes in proteins (Shahabadi and Hadidi 2014). In general, the increase in temperature causes the protein to change its three-dimensional arrangement, modifying its secondary and/or tertiary structure, which exposes the hydrophobic regions.

Generally, an increase in temperature causes an increase in adsorption capacity. In this study however the inverse occurred, which indicates that other variables affected this process. One of these variables was the saline concentration, which in this study was much higher than in previous experiments, e.g. Bonomo et al. (2006) and Ueberbacher et al. (2010). The effects of salt in solution on the interaction of the protein with adsorbents have been extensively investigated over several decades. Both of these studies indicate saline compounds increase the surface tension of the solution, increasing the molecular aggregation between proteins. This molecular aggregation can hide the hydrophobic sites that were exposed, reducing the hydrophobic interaction between the adsorbent and the adsorbate (Shahabadi and Hadidi 2014). In addition, the increase in temperature associated with high salt concentrations can cause elongation in the protein structure. Therefore, the interactions between hydrophobic regions of the protein were possibly reduced with the binding site of the adsorbent surface, reducing the interaction (Berezovskaya et al. 2013). These results are similar to Kundu et al. (2016), who studied the synergistic effect of temperature and salt concentration on protein adsorption and realized the increase in temperature increases the adsorption of this type of biomolecule when there is no salt in the solution. As the salt concentration increases however, there is a weak attraction between adsorbent and adsorbate.

Table 2 shows the adjusted parameters of the Langmuir model and the value of the coefficient of determination ( $R^2$ ). In all cases, the parameters were significant ( $p < 0.05$ ), and the determination coefficient equal to or greater than 0.91.

The Langmuir  $K_c$  isotherm parameter ( $\text{mL mg}^{-1}$ ) reflects the nature of the adsorbent material and can be used to compare the adsorption performance. This parameter is related to the interaction forces between the adsorbent and the adsorbent. Thus, the higher the value of this parameter the greater the probability of adsorption (Langmuir, 1916; Azizian et al. 2018). The results of this study however did not follow this direction, since the temperature of 318.15 K resulted in the highest  $K_c$  value ( $2.350 \text{ mL mg}^{-1}$ ) but not the highest adsorption value. Bonomo et al (2006) and Geçgel and Üner (2018), studying the adsorption of BSA on hydrophobic adsorbents, obtained  $K_c$  values in the

range of  $0.03\text{--}0.28 \text{ mL mg}^{-1}$  and  $0.0093\text{--}0.4352 \text{ mL mg}^{-1}$ , respectively.

This is because obtaining the  $K_c$  parameter does not take into account the saline concentration present in the solution. According to Langmuir (1916),  $K_c$  represents the affinity of the adsorbate for the binding site and assumes the forces are applied by atoms of unsaturated surfaces, therefore they do not extend more than the diameter of the adsorbed molecule and thus the adsorption is restricted to a monolayer. Therefore the high concentration of sodium sulfate, together with the increase in temperature, increased the size and diameter of the molecule. This fact interfered with the interaction between the hydrophobic zones of the protein and the adsorbent surface.

### Thermodynamic analysis

Based on the parameters studied, the hydrophobic interaction process became less favorable with the increase in temperature, which was verified by the reduction in saturation capacity adjusted in the Langmuir model. Conformational changes occurred in the protein used and configurational changes occurred throughout the system as a function of temperature. Thermodynamic analysis clarified these phenomena. The van't Hoff graph is presented in Fig. 6 and the estimated values for the variation of the standard thermodynamic properties of Gibbs free energy adsorption, enthalpy, and entropy (multiplied by Kelvin temperature) are shown in Fig. 7.

As shown in Fig. 7, the adsorption process was spontaneous ( $\Delta G^\circ < \text{zero}$ ) at all temperatures studied. There was a tendency to enthalpic-entropic compensation in the process, especially above 308.15 K.

The evaluated adsorption process tends to become exothermic with increasing temperature. At the two lowest

**Table 2** Fitted parameters of the isotherm models for BSA adsorption at different temperatures

Temperature (K)	$q_{\text{max}}$ ( $\text{mg g}^{-1}$ )	$K_c$ ( $\text{mL mg}^{-1}$ )	$R^2$
298.15	1735.56	1.001	0.95
308.15	1133.65	2.067	0.94
318.15	946.34	2.350	0.91
328.15	696.28	1.981	0.96

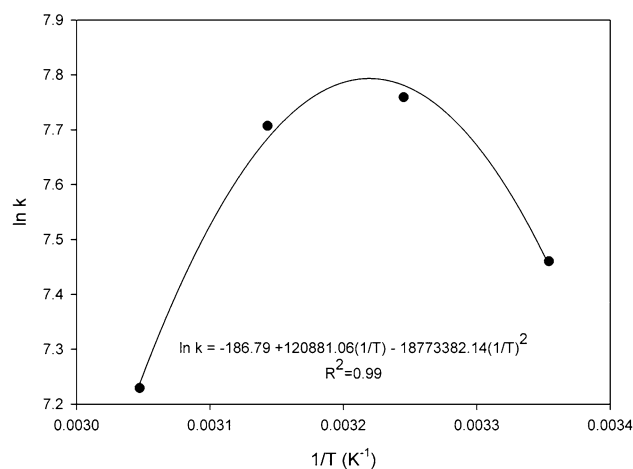


**Fig. 6** Van't Hoff graph for nonlinear analysis

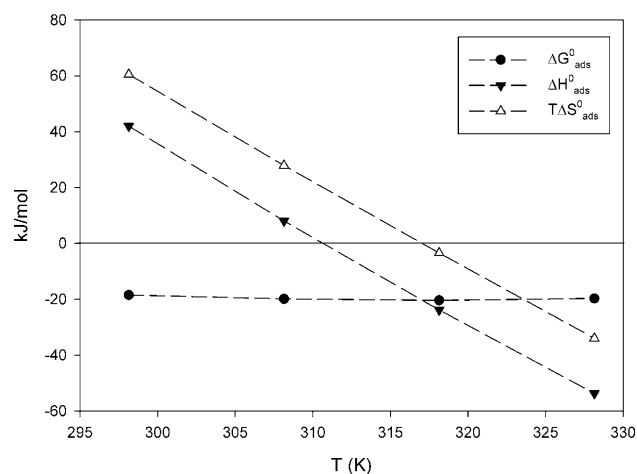


**Fig. 7** Thermodynamic properties as a function of temperature in the BSA adsorption process

temperatures evaluated (298.15 and 308.15 K), the process was entropically directed, becoming enthalpically directed at the other temperatures evaluated (318.15 and 328.15 K). This suggests that conformational changes in protein at lower temperatures promoted a greater exposure of hydrophobic groups for adsorption to occur, even though the process is not enthalpically advantageous, requiring energy (Chen et al. 2007). At higher temperatures, despite the adsorption process becoming interesting from an entrapment point of view, the BSA molecules may have acquired a configuration at such a denaturation level that, even with the exposure of hydrophobic groups to adsorption, they caused a greater spatial impediment on the active sites of the adsorbent, which reduced the configurational entropy of the system and consequently the amount of BSA adsorbed. This behavior is contrary to that reported in studies involving hydrophobic interaction (Chen et al. 2007; Unler 2013). This study however used a higher salt concentration than previous studies, which resulted in the increased hydrophobic effect. The combination of the high concentration of sodium sulfate with the increase in temperature may have promoted this characteristic (Bigman and Levy 2018).

## Conclusion

An adsorbent was produced with potential use in chromatographic techniques based on hydrophobic interaction focused on the purification and protein capture processes. The adsorbent was characterized for chromatographic applications and the functionalization process did not lead to significant differences in the analyzed parameters, except for the fraction of macropores and micropores that showed a difference between treatments. The adsorption capacity of the

BSA decreased as the temperature increased. The adjusted parameters of the Langmuir isotherm model were satisfactory and the non-linear van't Hoff analysis confirmed the spontaneous nature of the adsorption process.

**Funding** This work was supported by the State University of Southwest of Bahia (UESB) by labs access, Coordination for the Improvement of Higher Education Personnel (CAPES) by funding 819178/2015 and 88881.068456/2014-01 and National Council for Scientific and Technological Development (CNPq) by funding 303353/2018-7.

## Declarations

**Conflict of interest** The authors declare they have no known competing financial interests or personal relationships that could have appeared to influence the work reported in this paper.

## References

- Andaç M, Galaev IY, Denizli A (2016) Affinity based and molecularly imprinted cryogels: applications in biomacromolecule purification. *J Chromatogr B* 1021:69–80. <https://doi.org/10.1016/j.jchromb.2015.09.034>
- Asgari S, Jahanshahi M, Rahimpour A (2014) Cost-effective nanoporous agar-agar polymer/nickel powder composite particle for effective bio-products adsorption by expanded bed chromatography. *J Chromatogr A* 1361:191–202. <https://doi.org/10.1016/j.chroma.2014.08.016>
- Azizian S, Eris S, Wilson LD (2018) Re-evaluation of the century-old Langmuir isotherm for modeling adsorption phenomena in solution. *Chem Phys* 513:99–104. <https://doi.org/10.1016/j.chemphys.2018.06.022>
- Bayramoglu G, Arica MY (2021) Strong and weak cation-exchange groups generated cryogels films for adsorption and purification of lysozyme from chicken egg white. *Food Chem* 342:128295. <https://doi.org/10.1016/j.foodchem.2020.128295>
- Berezovskaya Y, Porrini M, Barran PE (2013) The effect of salt on the conformations of three model proteins is revealed by variable temperature ion mobility mass spectrometry. *Int J Mass Spectrom* 345–347:8–18. <https://doi.org/10.1016/j.ijms.2013.02.005>
- Bigman LS, Levy Y (2018) Entropy–enthalpy compensation in conjugated proteins. *Chem Phys* 514:95–105
- Bonomo RCF, Minim LA, Fontan RCI, Coimbra JSR (2006) Hydrophobic interaction adsorption of whey proteins: effect of temperature and salt concentration and thermodynamic analysis. *J Chromatogr B* 844:6–14
- Bradford MM (1976) Rapid and sensitive method for quantitation of microgram quantities of protein utilizing principle of protein-dye binding. *Anal Biochem* 72:248–254
- Carvalho BMA, da Silva LHM, Carvalho LM, Soares AM, Minim LA, da Silva SL (2013) Microcalorimetric study of the adsorption of lactoferrin in supermacroporous continuous cryogel with immobilized  $\text{Cu}^{2+}$  ions. *J Chromatogr A* 1312:1–9. <https://doi.org/10.1016/j.chroma.2013.08.042>
- Chen W, Liu Z, Lin P, Fang C, Yamamoto S (2007) The hydrophobic interactions of the ion-exchanger resin ligands with proteins at high salt concentrations by adsorption isotherms and isothermal titration calorimetry. *Sep Purif Technol* 54:212–219
- Chen F, Yao KJ, Shen S, Yun J (2008) Influence of grafting conditions on the properties of polyacrylamide-based cation-exchange cryogels grafted with 2-acrylamido-2-methyl-1-propanesulfonic



- acid. *Chem Eng Sci* 63:71–77. <https://doi.org/10.1016/j.ces.2007.09.008>
- Coates J (2006) Interpretation of infrared spectra: a practical approach. *Encyclopedia of analytical chemistry* (online). Wiley. <https://doi.org/10.1002/9780470027318.a5606>
- Da Silva JF, Silva DL, Nascimento RG, Veríssimo LAA, Veloso CM, Bonomo RCF, Fontan RCI (2019) Enhancements in sugar immobilization in polymeric macroporous matrices for affinity capture. *J Appl Polym Sci* 136:36–47
- Demirci S, Sahiner N (2021) Superporous neutral, anionic, and cationic cryogel reactors to improved enzymatic activity and stability of  $\alpha$ -glucosidase enzyme via entrapment method. *Chem Eng J* 409:128233. <https://doi.org/10.1016/j.cej.2020.128233>
- Ertürk G, Mattiasson B (2014) Cryogels-versatile tools in bioseparation. *J Chromatogr A* 1357:24–35. <https://doi.org/10.1016/j.chroma.2014.05.055>
- Fontan RCI, Bonomo RCF, Gonçalves GRF, Minim VPR, Minim LA (2018) Alternatives for characterizing macroporous polyacrylamide monolithic ion exchanger columns. *Polym Eng Sci* 58:1717–1725
- Geçgel Ü, Üner O (2018) Adsorption of bovine serum albumin onto activated carbon prepared from elaeagnus stone. *Bull Chem Soc Ethiop* 32(1):53–63
- Gonçalves GRF, Gandolfi ORR, Santos LS, Bonomo RCF, Veloso CM, Veríssimo LAA, Fontan RCI (2016) Development of supermacroporous monolithic adsorbents for purifying lectins by affinity with sugars. *J Chromatogr B* 1033–1034:406–412
- Gonçalves GRF, Gandolfi ORR, Santos LS, Bonomo RCF, Veloso CM, Veríssimo LAA, Fontan RCI (2017) Immobilization of sugars in supermacroporous cryogels for the purification of lectins by affinity chromatography. *J Chromatogr B* 1068–1069:71–77
- Guo X, Li X, Jiang Y, Yi L, Wu Q, Chang H, Diao X, Sun Y, Pan X, Zhou N (2014) A spectroscopic study on the interaction between *p*-nitrophenol and bovine serum albumin. *J Lumin* 149:353–360
- Ingavle GC, Baillie LWJ, Zheng Y, Lis EK, Savina IN, Howell CA, Mikhailovsky SV, Sandeman SR (2015) Affinity binding of antibodies to supermacroporous cryogel adsorbents with immobilized protein A for removal of anthrax toxin protective antigen. *Biomaterials* 50:140–153. <https://doi.org/10.1016/j.biomaterials.2015.01.039>
- Jungbauer A (2005) Chromatographic media for bioseparation. *J Chromatogr A* 1065:3–12. <https://doi.org/10.1016/j.chroma.2004.08.162>
- Kumar A, Bansal V, Andersson J, Roychoudhury P, Mattiasson B (2006) Supermacroporous cryogel matrix for integrated protein isolation. Immobilized metal affinity chromatographic purification of urokinase from cell broth of a human kidney cell line. *J Chromatogr A* 1103:35–42
- Kundu S, Aswal VK, Kohlbrecher J (2016) Synergistic effect of temperature, protein and salt concentration on structures and interactions among lysozyme proteins. *Chem Phys Lett* 657:90–94. <https://doi.org/10.1016/j.cplett.2016.05.066>
- Langmuir I (1916) The dissociation of hydrogen into atoms. III. The mechanism of the reaction. *J Am Chem Soc* 38:1145–1156
- Mól PCG, Veríssimo LAA, Eller MR, Minim VPR, Minim LA (2017) Development of an affinity cryogel for one step purification of lysozyme from chicken egg white. *J Chromatogr B* 1044–1045:17–23
- Nascimento IS, Silva DL, Pereira TB, Gonçalves GRF, Veríssimo LAA, Veloso CM, Bonomo RCF, Fontan RCI (2019) Single-step purification of lectins from jackfruit (*Artocarpus integrifolia*) seeds using a supermacroporous ion exchange cryogel. *Rev Mex Ing Quim* 18:313–324
- Oliveira ACF, Neves ICO, Saraiva JAM, Carvalho MFF, Batista GA, Veríssima LAA, Resende JA (2019) Capture of lysozyme on macroporous cryogels by hydrophobic affinity chromatography. *Sep Sci Technol* 55(11):2012–2024
- Osman B, Sagdılek E, Gümrükçü M, Sarıkayaa AG (2019) Molecularly imprinted composite cryogel for extracorporeal removal of uric acid. *Colloids Surf B* 183:110456. <https://doi.org/10.1016/j.colsurfb.2019.110456>
- Plieva FM, Andersson J, Galaev IY, Mattiasson B (2004) Characterization of polyacrylamide based monolithic columns. *J Sep Sci* 27:828–836
- Plieva FM, Galaev IY, Noppe W, Mattiasson B (2008) Cryogel applications in microbiology. *Trends Microbiol* 16:543–551. <https://doi.org/10.1016/j.tim.2008.08.005>
- Plieva FM, Seta E, Galaev IY, Mattiasson B (2009) Macroporous elastic polyacrylamide monolith columns: processing under compression and scale-up. *Sep Purif Technol* 65:110–116
- Rimdisut S, Somsaeng K, Kewsuwan P, Jubsilp C, Tiptipakorn S (2012) Comparison of gamma radiation crosslinking and chemical crosslinking on properties of methylcellulose hydrogel. *Eng J* 16:21–32. <https://doi.org/10.4186/ej.2012.16.4.15>
- Sahiner N (2018) Super macroporous poly(*N*-isopropyl acrylamide) cryogel for separation purpose. *Polym Adv Technol* 29:2184–2191. <https://doi.org/10.1002/pat.4326>
- Savina IN, Mattiasson B, Galaev IY (2005) Graft polymerization of acrylic acid onto macroporous polyacrylamide gel (cryogel) initiated by potassium diperiodatocuprate. *Polymer* 46:9596–9603
- Shahabadi N, Hadidi S (2014) Molecular modeling and spectroscopic studies on the interaction of the chiral drug venlafaxine hydrochloride with bovine serum albumin. *Spectr Acta Part A Mol Biomol Spectr* 122:100–106
- Türkmen D, Denizli A (2014) PHEMA based composite cryogels with loaded hydrophobic beads for lysozyme purification. *Colloids Surf B Biointerfaces* 123:859–865. <https://doi.org/10.1016/j.colsurfb.2014.10.034>
- Ueberbacher R, Rodler A, Hahn R, Jungbauer A (2010) Hydrophobic interaction chromatography of proteins: thermodynamic analysis of conformational changes. *J Chromatogr A* 1217:184–190
- Unler OB (2013) Preparation of a novel hydrophobic affinity cryogel for adsorption of lipase and its utilization as a chromatographic adsorbent for fast protein liquid chromatography. *AIChE* 28:33–39. <https://doi.org/10.1002/btpr.1863>
- Veríssimo LAA, Paganoto FS, Mol PCG, Fontan RCI, Minim VPR, Minim LA (2017) Preparation of an affinity cryogel column for lysozyme purification. *Sep Sci Technol* 52:1973–1982
- Wang C, Dong XY, Jiang Z, Sun Y (2013) Enhanced adsorption capacity of cryogel bed by incorporating polymeric resin particles. *J Chromatogr A* 1272:20–25. <https://doi.org/10.1016/j.chroma.2012.11.059>
- Wen L, Liua L, Wang X, Wang ML, Lin JM, Zhao RS (2020) Spherical mesoporous covalent organic framework as a solid-phase extraction adsorbent for the ultrasensitive determination of sulfonamides in food and water samples by liquid chromatography-tandem mass spectrometry. *J Chromatogr A* 1625:46–52. <https://doi.org/10.1016/j.chroma.2020.461275>
- Yao K, Shen S, Yun J, Wang L, He X, Yu X (2006) Characterization of a novel continuous supermacroporous monolithic cryogel embedded with nanoparticles for protein chromatography. *J Chromatogr A* 1109:103–110

**Publisher's Note** Springer Nature remains neutral with regard to jurisdictional claims in published maps and institutional affiliations.